Journal of Chemical Health Risks
www.jchr.org
JCHR (2025) 15(4), 2763-2772 | ISSN:2251-6727

Synthesis and Characterization of "Keratin-Alginate/ZnO Nanogel: An Innovative Antimicrobial System for Enhanced Wound Healing "

Singhai, Akansha[1]; Narkhede, Snehal[1]; Phillips, Enosh[1,3]; Dadsena, Ashish[1]; Sahu, Reecha[2*]; Sur, Arunima[1]; Kush Kumar Nayak[4]

[1]Amity Institute of Biotechnology, Amity University Chhattisgarh, India

[2]Biomedical Engineering and Bioinformatics, University Teaching Department, Chhattisgarh Swami Vivekanand Technical University, India

Formally, affiliated to Amity Institute of Biotechnology, Amity University Chhattisgarh

[3]St. Aloysius College, Jabalpur, India

[4]School of Studies in Biotechnology, Shaheed Mahendra Karma Vishwavidyalaya, Bastar, India

Formally, affiliated to Amity Institute of Biotechnology, Amity University Chhattisgarh

Corresponding Author: Reecha Sahu,

(Received: 16 June 2025 Revised: 20 July 2025 Accepted: 19 August 2025)

KEYWORDS
Keratin , alginate , nanogel , antimicrobial, wound healing, biomaterial.

ABSTRACT:
Biomaterials, whether naturally derived or synthetic, are engineered to enhance cellular interactions, promote tissue regeneration, and ensure biocompatibility, making them highly promising for advanced wound healing applications. Among them, keratin-based nanogels represent a novel class that utilizes keratin's intrinsic bioactivity to form three-dimensional scaffolds conducive to cell attachment and tissue remodeling. The incorporation of alginate, a natural anionic polysaccharide, further enhances these nanogels by imparting structural integrity, improved mechanical strength (~15–20 kPa), and high moisture retention (~85%), essential for an optimal wound environment.
In this study, keratin–alginate nanogels were synthesized via ionic crosslinking and comprehensively characterized. Fourier-transform infrared spectroscopy (FTIR) confirmed crosslinking through characteristic amide I (~1650 cm^{-1}) and carboxylate (~1600 cm^{-1}) peaks. X-ray diffraction (XRD) analysis revealed a semi-crystalline nature, supporting structural stability. Field-emission scanning electron microscopy (FESEM) showed a porous, interconnected morphology (pore size ~50–150 µm), favorable for nutrient diffusion and cell infiltration. Porosity and water absorption studies demonstrated excellent uptake (up to 900% of dry weight), while water retention analysis confirmed prolonged moisture maintenance. In vitro degradation assays indicated controlled degradation suitable for tissue remodeling. Additionally, antimicrobial investigations demonstrated strong activity against common wound pathogens, enhancing infection protection. The synergistic effects of keratin and alginate improve mechanical, physicochemical, and biological properties, supporting potential therapeutic delivery. Overall, keratin–alginate nanogels present a multifunctional platform for advanced wound healing and regenerative medicine applications.

1. Introduction: Protein-based polymers in biomedical applications has seen increasing interest due to their inherent properties, such as biocompatibility, biodegradability, functional versatility, bioactivity ability to closely resemble extracellular matrix (ECM) facilitates interactions with cellular integrins, promoting cellular integrins, essential for effective wound healing (Sellappan & Manoharan, 2024). The presence of intrinsic cell-binding motifs that facilitate cell adhesion, proliferation, and migration. Keratin, in particular, has emerged as a versatile biomaterial, especially valuable in wound healing applications. Keratin is a fibrous protein abundantly found in biological tissues such as hair, wool, and feathers. Its high cysteine content contributes to the

Journal of Chemical Health Risks
www.jchr.org
JCHR (2025) 15(4), 2763-2772 | ISSN:2251-6727

formation of strong disulfide bonds, resulting in a stable and highly ordered polypeptide structure. Beyond its structural role, keratin is increasingly recognized for its biomedical potential, particularly in wound healing, where it supports epithelialization and modulates inflammatory responses. Keratin can also be processed into diverse scaffolds—including films, sponges, hydrogels, nanogels, microcapsules, and microspheres—broadening its applications in regenerative medicine (Qian et al., 2020).

Alginate, a natural anionic polysaccharide , a linear copolymer consists of homopolymeric blocks of (1-4)-linked β-D-mannuronate (M) and its C-5 epimer, α-L-guluronate (G), covalently linked in varying sequences or block patterns. It is derived from brown seaweed (*Phaeophyceae*) including *Laminaria* or *Ascophyllum nodosum*. Owing to its excellent biocompatibility, biodegradability, and gel-forming ability, alginate is widely employed in biomedical applications, particularly in combination with keratin to produce composite biomaterials.

The development of the ALG/KER blend film was driven to create a novel material that synergistically combines the functional and structural properties of both polymers, enhancing their potential applications (Moholkar et al., 2021a) .The application of the blend film can vary as per its characteristics such as 1) They can provide an optimal moist environment for wound healing, facilitate cellular proliferation, and support tissue regeneration due to their controlled water-retention capacity and biocompatibility.2) The blend can be engineered for sustained and targeted drug release for therapeutic applications. 3) Supports cell attachment, scaffolding and growth for tissue repair. 4) The blend can be utilized in s cosmetic products for hydration, healing, and rejuvenation. It can also be ideal in laminating films to retain moisture in fruits for enhancing their shelf life. 5) Their biodegradable nature supports their use in sustainable food packaging and edible coatings. Overall, by combining keratin's bioactivity with alginate's mechanical and gel-forming properties, these blends achieve a balance of strength, flexibility, biocompatibility, and water management, making them highly adaptable for both therapeutic and industrial applications.

Recent research has increasingly emphasized on synthesizing keratin-based nanogels that leverage the protein's favourable characteristics while enhancing its functionality through nanotechnology. Nanogels, three-dimensional cross-linked polymer networks with nanoscale dimensions, offer several advantages for wound healing applications. Their high surface area-to-volume ratio allows for efficient loading and controlled release of bioactive molecules, while their porous structure facilitates cell infiltration and nutrient exchange. To validate their structural and functional properties, these nanogels are commonly characterized using advanced analytical techniques. X-ray diffraction (XRD) is employed to assess crystallinity, Fourier-transform infrared spectroscopy (FTIR) provides information on molecular interactions, and field-emission scanning electron microscopy (FESEM) is used to examine surface morphology(Shanmugasundaram et al., 2018a).

The objective is to explore the synthesis and characterization of keratin-based nanogels for enhanced wound healing. These nanogels are evaluated for their cytocompatibility, anti-inflammatory potential, and ability to accelerate wound closure. In addition, comprehensive physicochemical analyses are carried out to establish the relationship between their structural features and functional performance, thereby providing deeper insight into their suitability as effective biomaterials for wound care.

Materials and Methods

The polymers used in this study included sodium alginate (ALG) in its sodium salt form (91% food grade), procured from LOBA Chemie (Mumbai, India), and keratin (KER), which was extracted in-house from chicken feathers collected at the local market in Jabalpur, Madhya Pradesh, India. Other reagents employed in the experiments were of analytical grade and sourced commercially: Tris-HCl (Tris Hydrochloride, mol. wt. 157.60) and 2-mercaptoethanol (mol. wt. 78.13) from LOBA Chemie; sodium dodecyl sulfate (SDS, mol. wt. 288.38) and urea (mol. wt. 60.06) from Merck (Whitehouse Station, NJ, USA). Milli-Q water was used for all experimental procedures.

Journal of Chemical Health Risks
www.jchr.org
JCHR (2025) 15(4), 2763-2772 | ISSN:2251-6727

1.1. Methods:

1.1.1. Fabrication of the nanogel:

Preparation of ALG-KER /ZnO nanogel :A stock solution of ALG (3 % w/v) homogenized using a magnetic stirrer at 50°C for 8 h. after which it was then stored at room temperature. Keratin (KER) was extracted from chicken feathers following the procedure described by Yamauchi et al. A KER stock solution (7% w/v) was subsequently homogenized using a magnetic stirrer at 60°C for 10 hours and was left at room temperature for 4 days. (Xie et al., 2018) The concentration of KER was kept higher than ALG to enable the study of KER's effect on biopolymer development. To prepare the ALG/KER blends, the keratin solution was gradually added to the alginate solution in predetermined volume ratios. The resulting mixtures were then homogenized using a magnetic stirrer for 2 h to obtain uniform composite solutions.

Next, As shown in figure.1 ZnO nanoparticles, prepared at a concentration of 1 mg/mL, were incorporated into the ALG/KER mixture. The pH of the solution was adjusted to 12–13 by the gradual addition of 1N sodium hydroxide (NaOH). o induce crosslinking and nanogel formation, 6 mL of a 25% glutaraldehyde solution was slowly added under continuous stirring. The blend was then maintained at 55 °C with constant stirring for 3 h to ensure complete homogenization. The resulting mixtures were then cast into Teflon-coated plastic boxes (85 × 50 × 20 mm³) and allowed to air-dry at ambient temperature. Once semi-transparent films formed, they were carefully removed from the boxes and allowed to further dried at room temperature to achieve complete drying (Zhai et al., 2018).

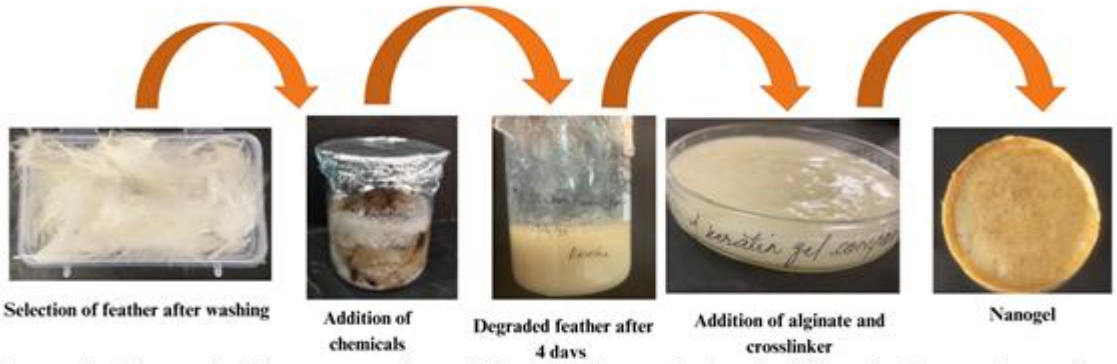

Figure 1. Schematic Representation of Feather Degradation for Keratin Extraction and ALG-KER /ZnO Scaffold Fabrication.

1.1.2. Fabrication of ZnO NPs

In this study, we optimized our previously established green synthesis protocol to fabricate zinc oxide nanoparticles (ZnO NPs) using *Moringa oleifera* leaf extract. The extract served as a natural reducing and stabilizing agent, providing bioactive compounds and creating an alkaline medium conducive to ZnO NP formation. Following the synthesis reaction, the nanoparticles were allowed to settle, then repeatedly washed and dried to yield the final product (Khorasani et al., 2021).

2. Analytical analysis

2.1. Field Emission Scanning Electron Microscopy (FESEM)

Field Emission Scanning Electron Microscopy (FESEM) was utilized to examine the surface morphology and structural characteristics of the synthesized nanogel. This technique provided high-resolution imaging, enabling visualization of the microstructural details such as surface texture, pore distribution, and overall morphology. Such observations are essential for correlating the physical characteristics of the nanogels with their functional performance in biomedical applications (Moholkar et al., 2021b).

2.2. X-ray diffraction (XRD)

X-Ray Diffraction (XRD) was carried out to determine the crystalline structure of the nanogel, offering

Journal of Chemical Health Risks
www.jchr.org
JCHR (2025) 15(4), 2763-2772 | ISSN:2251-6727

information on its molecular organization and phase composition. This technique enabled the identification of distinct crystalline phases, the extent of crystallinity, and the presence of amorphous regions . Such structural insights are crucial for assessing the nanogel's stability, mechanical behavior, and potential interactions in various applications (Shanmugasundaram et al., 2018b).

2.3. Fourier Transform Infrared Spectroscopy (FTIR)

FTIR was applied to identify the functional moieties and confirm the chemical structure of the nanogel. This technique detected specific chemical bonds, verifying the incorporation of keratin and alginate into the nanogel matrix. The FTIR spectra revealed characteristic absorption bands corresponding to various functional groups, confirming that the intended chemical modifications were successfully achieved (Salleh & Abd Rashid, 2024a).

2.4. *In vitro* degradation of the scaffold:

The *in vitro* degradation was evaluated by verifying the percent of weight loss of the scaffold in phosphate buffer saline (PBS) solution. The scaffolds were sliced into uniform pieces (10x10x2 mm^3) and immersed in PBS within sealed containers, followed by incubation in a shaking incubator at 37 °C. The samples were collected in duplicates after 1st, 2nd, and 3rd week and dried at ambient temperature for 24 hours, after that its dry weight was measured. The percentage of weight loss was calculated using the following equation .

$$Weight\ Loss\ (\%) = \frac{Wi - Wt}{Wi} \text{X}\ 100$$

where, Wi was a dry weight at the initial time, and Wt was a dry weight of the scaffold at time 't'.

The percentage of weight loss of the keratin/alginate scaffold measured after 1st, 2nd, and 3rd week was found 19.14±5.13 %, 52.97±10.03 %, and 62.64±6.96 %, respectively. Approximately, After 3 weeks, approximately 37% of the scaffold's original weight remained of *in vitro* degradation. These findings indicate that the fabricated scaffold has the ability to degrade under *in vitro* or *in vivo* applications. Although, the scaffolds, get degraded *in vitro*, but still are able to maintain its shape and structure after 3rd week under static (non-stirring) condition of degradation treatment. Dissolution of alginate and keratin in PBS causes the weight loss of the scaffold in due course of the study period. Ultimately, scaffold gets broken into smaller part and provides a larger surface area for degradation, which is again useful for the cell proliferation and tissue growth (Feroz et al., 2020).

2.5. Water retention capacity of the scaffold

The ability of the scaffold to retain water reflects its hydrophilic nature (Rajabi et al., 2020). The water retention capacity of the scaffold was calculated by the following equation:

$$\text{W}_\text{R} = \frac{W2 - W1}{w1}\ X\ 100$$

W1= dry weight, and W2 = weight of the scaffold after soaked in water

2.6. Antimicrobial Investigation

The antimicrobial efficacy of four scaffold formulations was assessed against *Staphylococcus aureus*, *Pseudomonas* spp., *Escherichia coli*, and *Enterobacter* spp. Test groups consisted : (i) a 30 µg tetracycline control, (ii) keratin discs, (iii) keratin with 7% alginate, and (iv) keratin–alginate incorporated with ZnO nanoparticles. Nutrient agar plates were inoculated with standardized bacterial suspensions, and discs were placed aseptically. After 24 hours of incubation at 37 °C, zones of inhibition were measured using a digital Vernier caliper. Each experiment was performed in triplicate, and data were expressed as mean ± SD for statistical reliability (Kakkar et al., 2014).

3. Results and discussion

3.1. Morphological Analysis

FESEM analysis revealed key structural features of the synthesized materials. Figure 2(A), captured at 5000x magnification, shows the extracted keratin exhibiting a rough, fibrous morphology, indicative of effective feather degradation and protein fiber disorganization typical of chemically extracted keratin . At higher magnification (50,000x), Fig. 2(B) displays needle-like crystalline fragments embedded in the protein matrix, suggesting partial crystallinity induced by chemical treatment .

Figure 2(C), at 10,000x magnification, illustrates the keratin–alginate/ZnO nanogel, where keratin fibers are uniformly distributed within the alginate matrix, forming a cohesive and interconnected network (Wang et al.,

Journal of Chemical Health Risks
www.jchr.org
JCHR (2025) 15(4), 2763-2772 | ISSN:2251-6727

2023). This structural uniformity indicates successful incorporation of ZnO

nanoparticles and homogenous blending of components, crucial for mechanical stability and functional performance. At 98,970× magnification, Fig. 2(D) further confirms the nanoscale integration of ZnO within the keratin–alginate matrix, with smooth, intact fiber surfaces and no visible phase separation.

Overall, the morphological data confirm the successful synthesis of a structurally stable keratin–alginate/ZnO nanogel, with features that support its potential in antimicrobial applications and biomedical applications (Bhat et al., 2024).

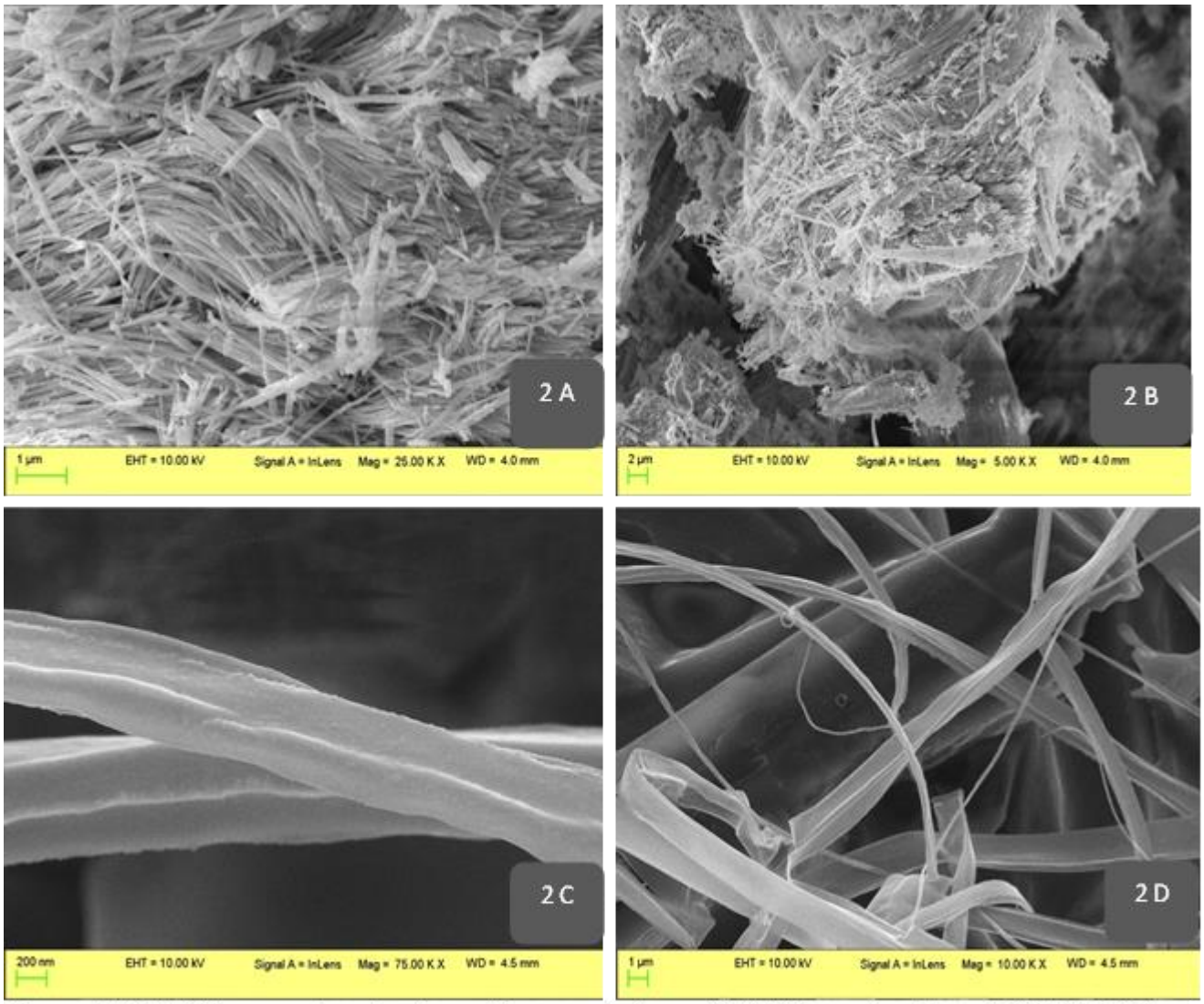

Figure. 1 FESEM images showing the surface morphology of (A, B) pure keratin and (C, D) ALG-KER/ZnO nanogel.

3.2. XRD Analysis

X-ray diffraction analysis verified the crystalline characteristics of the extracted keratin, with prominent peaks at 2θ = 22°, 25°, 30°, 32°, 36°, 38°, and 42°, indicating well-defined molecular arrangements. Peaks at 2θ = 22° and 32° correspond to α-helix and β-sheet structures, respectively, with the predominance of β-sheet structures highlighting the intrinsic structural complexity of keratin (Sarma, 2022).

Journal of Chemical Health Risks
www.jchr.org
JCHR (2025) 15(4), 2763-2772 | ISSN:2251-6727

In the composite nanogel, a broad peak around 2θ = 22°–25° indicated in figure 3 the semicrystalline nature of alginate. Sharp peaks at 2θ = 30°, 35°, 38°, 42°, 50°, 58°, and 70° confirmed the presence of ZnO nanoparticles with a hexagonal wurtzite structure . These results collectively validate the successful integration of ZnO into the keratin–alginate matrix, forming a structurally robust nanogel (Mujeeb Rahman et al., 2018).

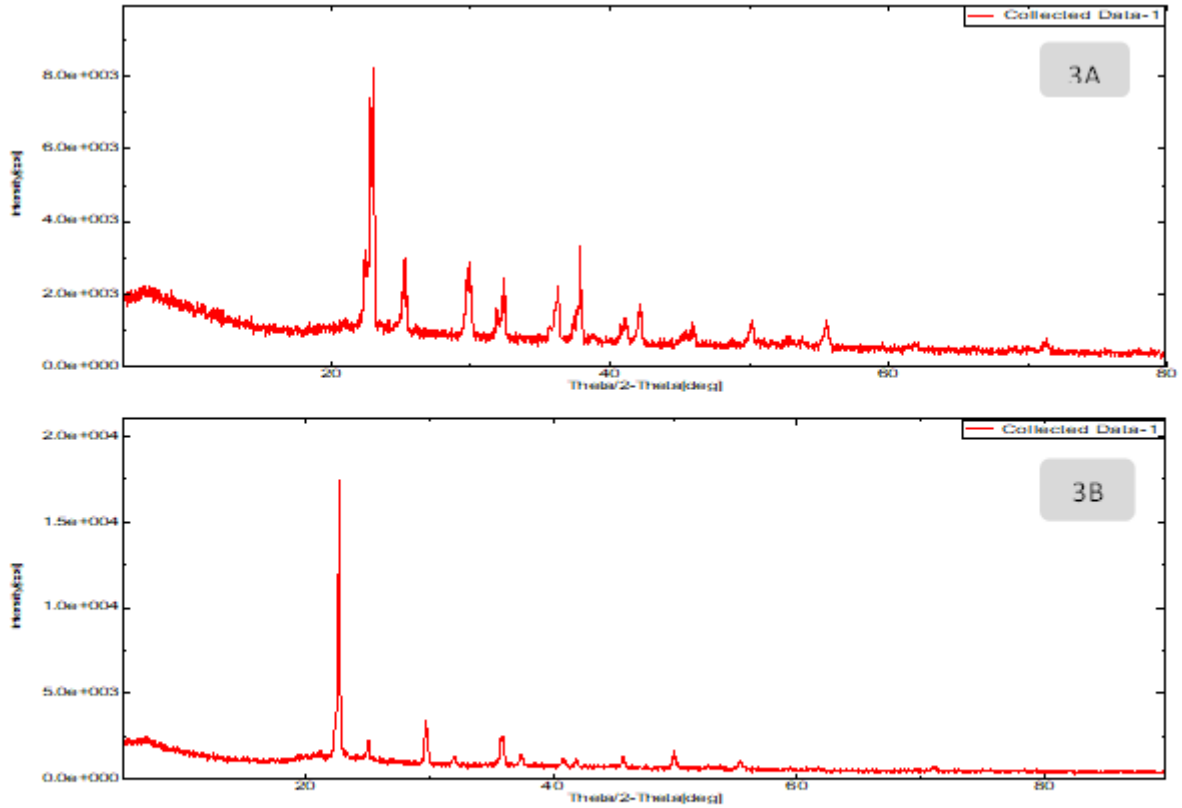

Figure 1: X-ray diffraction (XRD) analysis of (A) keratin and (B) keratin-ALG/ZnO nanogel.

3.3. FTIR Analysis

FTIR spectroscopy was employed to characterize the chemical structure of extracted keratin (Fig. 4A), with spectra recorded in the 3600–600 cm^{-1} range. A prominent peak at 3332 cm^{-1} corresponds to N–H stretching of peptide bonds (–CO–NH–), while peaks at 1664, 1591, and 1457 cm^{-1} represent amide I, II, and III bands, respectively, indicating the presence of α-helix and β-sheet structures. The band at 1149 cm^{-1} indicates –OH stretching of carboxylic acids, and peaks in the 702–600 cm^{-1} region correspond to N–H bending, suggesting the presence of amino acids such as glutamine, cysteine, and threonine (Vikas et al., 2024). These results confirm that the extracted keratin is predominantly composed of β-sheet conformations with fewer α-helices.

Figure 4(B) presents the FTIR spectrum of the keratin–alginate/ZnO nanogel. Characteristic peaks of alginate were observed at ~3328 cm^{-1} (O–H stretching), 2920 cm^{-1} (C–H stretching), 1590 and 1410 cm^{-1} (asymmetric and symmetric COO^- stretching), and 1024 cm^{-1} (C–O–C stretching) . A distinct peak at 535 cm^{-1}, attributed to Zn–O stretching, confirms the successful incorporation of ZnO nanoparticles into the keratin–alginate matrix. Collectively, the FTIR data validate the chemical integrity of the nanogel and the formation of stable interactions among keratin, alginate, and ZnO (Karpuraranjith & Thambidurai, 2017).

Journal of Chemical Health Risks
www.jchr.org
JCHR (2025) 15(4), 2763-2772 | ISSN:2251-6727

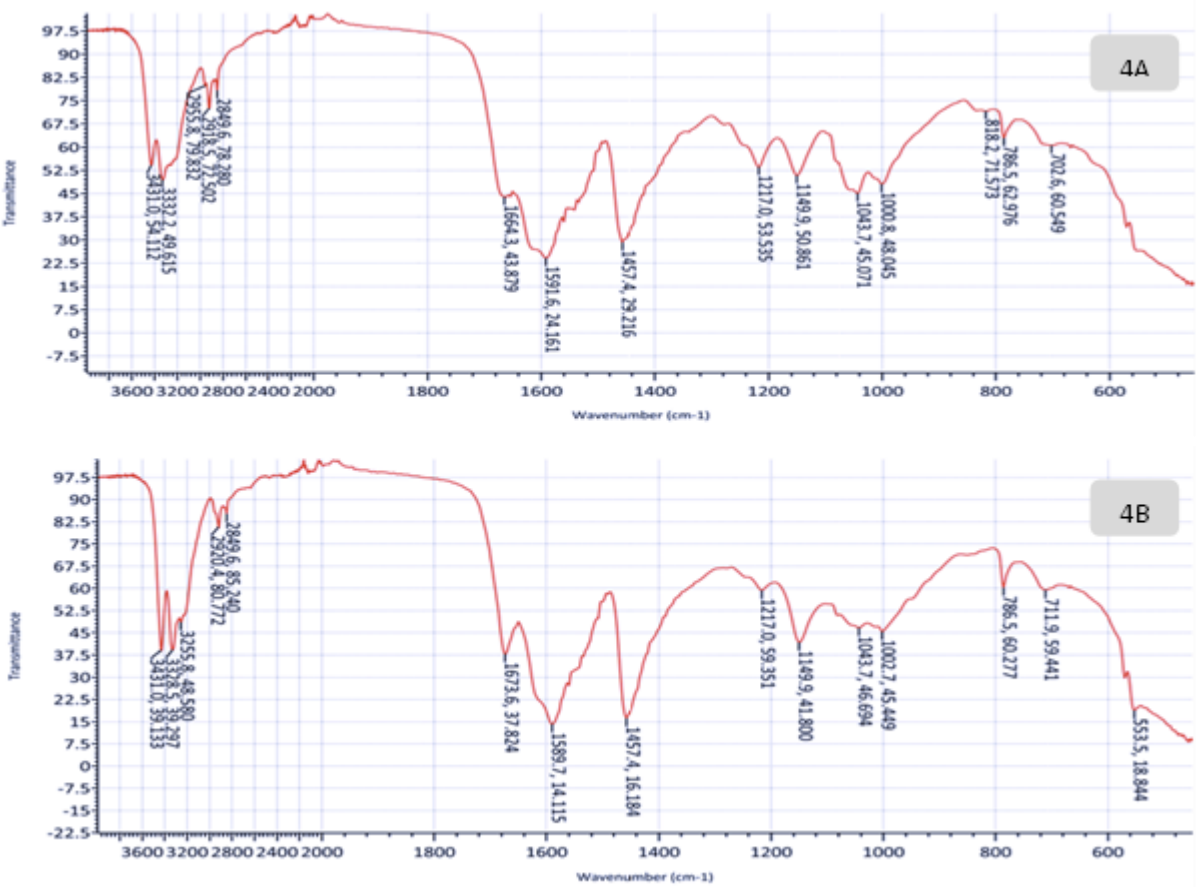

Figure 1. XRD of (A) keratin and (B) keratin-ALG/ZnO nanogel.

3.4. Degradation Study of the scaffold

The biodegradability of the scaffold was evaluated by measuring its percentage weight loss over time upon incubation in phosphate-buffered saline (PBS). The film exhibited progressive degradation, with weight loss recorded as 18.27 ± 1.25% (week 1), 47.73 ± 2.39% (week 2), 56.31 ± 1.23% (week 3), and 63.61 ± 3.07% (week 4). By the end of the fourth week, approximately 64% of the initial mass had degraded. This substantial degradability underscores the film's environmental compatibility and its suitability for biomedical applications. In tissue engineering, such degradable materials are preferred for temporary support, allowing cellular infiltration and extracellular matrix deposition, rather than remaining as permanent implants (Cleetus et al., 2020) .

3.5. Water Retention Capacity of the Blend Film

The fabricated blend film demonstrated a water retention capacity of 168 ± 5.94%, highlighting its strong hydrophilic nature. This inherent water affinity supports its potential use in biomedical applications such as nanogel for drug delivery and wound treatment, scaffolds for tissue regeneration (Shubha et al., 2024), and coatings designed to maintain moisture in sensitive environments (Raguvaran et al., 2017).

3.6. Antimicrobial Analysis of Keratin–Alginate/ZnO Nanogel

The antimicrobial efficacy of the synthesized keratin–alginate/ZnO nanogel was assessed using the zone of inhibition assay against multiple bacterial strains. The nanogel exhibited pronounced antibacterial activity, with inhibition zones (measured in mm) indicating substantial efficacy. Remarkably, the nanogel outperformed or matched the standard antibiotic tetracycline (30 µg), particularly against *Pseudomonas aeruginosa* and *Staphylococcus aureus*, both known for their resistance to conventional antibiotics (Salleh & Abd Rashid, 2024b). Figure 5 illustrates the antimicrobial activity of the developed nanogel against various pathogenic

Journal of Chemical Health Risks
www.jchr.org
JCHR (2025) 15(4), 2763-2772 | ISSN:2251-6727

strains: Fig. 5(A) shows inhibition against *Enterobacter*; Fig. 5(B) depicts *Pseudomonas aeruginosa*; Fig. 5(C) demonstrates activity against *Staphylococcus aureus*; and Fig. 5(D) displays inhibition of *Escherichia coli*, confirming its potent antibacterial action. These results align with recent studies demonstrating the effectiveness of natural polymer-based nanogels in disrupting bacterial growth and biofilm formation . Additionally, previous reports on enzyme-responsive nanogels for antibacterial phototherapy and wound healing support the clinical relevance of such systems (Pensalfini et al., 2017).

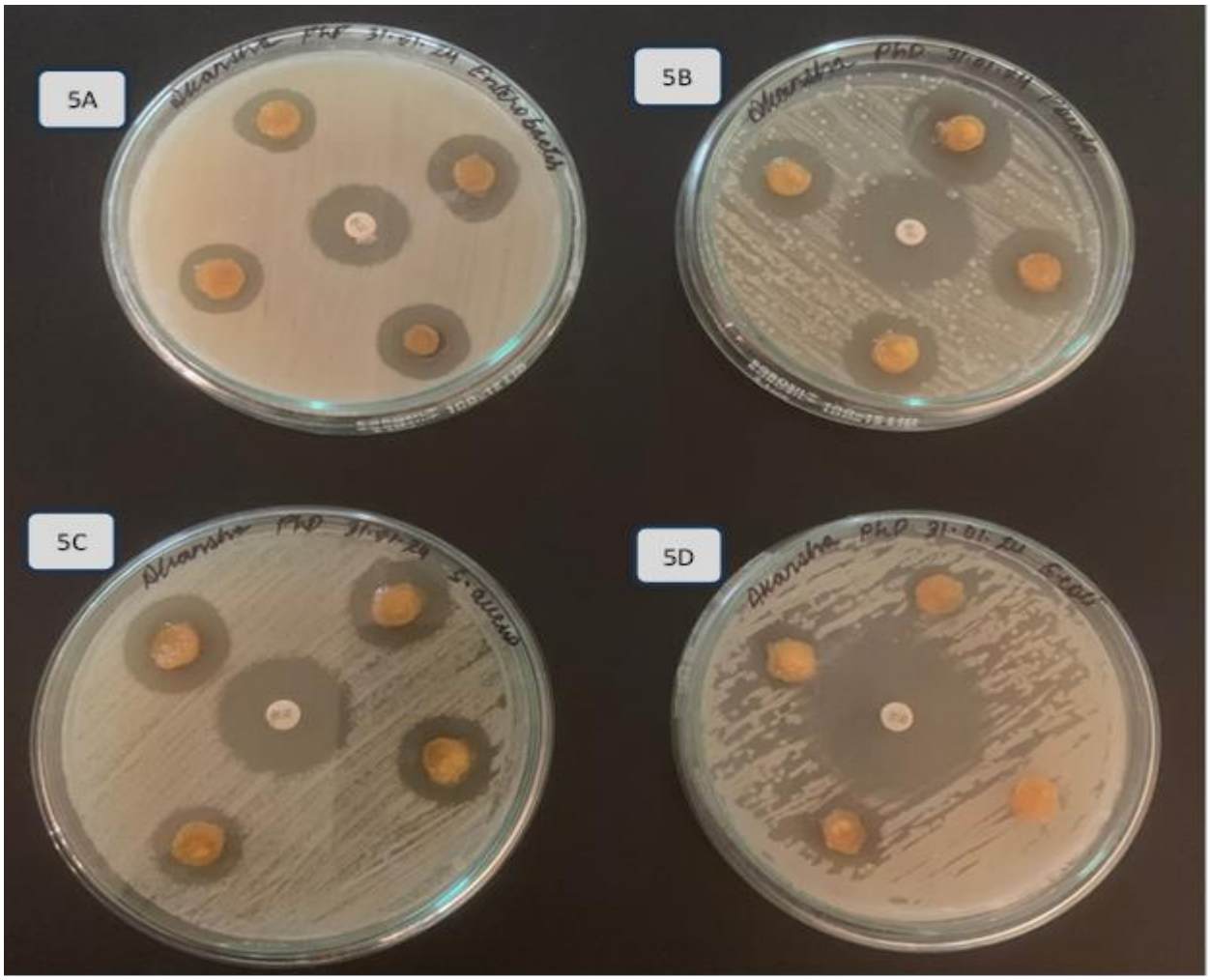

Figure 5. Antimicrobial activity of the keratin–alginate/ZnO nanogel evaluated against *Enterobacter* (A), *Pseudomonas aeruginosa* (B), *Staphylococcus aureus* (C) and *Escherichia coli* (D).

The enhanced antimicrobial performance is primarily attributed to the presence of ZnO nanoparticles, known for their broad-spectrum antibacterial activity. Overall, the findings underscore the potential of keratin–alginate/ZnO nanogels as promising agents for biomedical applications, particularly in combating multidrug-resistant infections and biofilms.

5. Conclusions

A series of KER-ALG/ZnO nanogel were successfully fabricated by the solution casting method. Structural and

Journal of Chemical Health Risks
www.jchr.org
JCHR (2025) 15(4), 2763-2772 | ISSN:2251-6727

physicochemical analyses, including XRD, SEM, and other characteristics like degradation rate, and the water retention capacity of the blend film revealed that polymer compatibility exists between ALG and KER and that the blend expresses the combined properties of their native polymers. The results demonstrated that the blend retains the complementary properties of both native polymers and exhibits sufficient tensile strength for biomedical use. These findings suggest that KER–ALG films can serve as versatile substrates for the development of advanced biomaterials, including drug delivery carriers, nanogels, and scaffolds for tissue engineering and regenerative medicine.

References

[1] Bhat, H. F., Amin, N., Nasir, Z., Nazir, S., Bhat, Z. F., Malik, A. A., Ganai, N. A., Andrabi, S. M., Shah, R. A., & Aadil, R. M. (2024). Keratin as an effective coating material for in vitro stem cell culture, induced differentiation and wound healing assays. *Heliyon*, *10*(5).

[2] Cleetus, C. M., Alvarez Primo, F., Fregoso, G., Lalitha Raveendran, N., Noveron, J. C., Spencer, C. T., Ramana, C. V, & Joddar, B. (2020). Alginate hydrogels with embedded ZnO nanoparticles for wound healing therapy. *International Journal of Nanomedicine*, 5097–5111.

[3] Feroz, S., Muhammad, N., Ratnayake, J., & Dias, G. (2020). Keratin-Based materials for biomedical applications. *Bioactive Materials*, *5*(3), 496–509.

[4] Kakkar, P., Verma, S., Manjubala, I., & Madhan, B. (2014). Development of keratin–chitosan–gelatin composite scaffold for soft tissue engineering. *Materials Science and Engineering: C*, *45*, 343–347.

[5] Karpuraranjith, M., & Thambidurai, S. (2017). Synergistic effect of chitosan-zinc-tin oxide colloidal nanoparticle and their binding performance on bovine albumin serum. *Materials Chemistry and Physics*, *199*, 370–378. https://doi.org/https://doi.org/10.1016/j.matchemphys.2017.07.019

[6] Khorasani, M. T., Joorabloo, A., Adeli, H., Milan, P. B., & Amoupour, M. (2021). Enhanced antimicrobial and full-thickness wound healing efficiency of hydrogels loaded with heparinized ZnO nanoparticles: In vitro and in vivo evaluation. *International Journal of Biological Macromolecules*, *166*, 200–212. https://doi.org/https://doi.org/10.1016/j.ijbiomac.2020.10.142

[7] Moholkar, D. N., Sadalage, P. S., Peixoto, D., Paiva-Santos, A. C., & Pawar, K. D. (2021a). Recent advances in biopolymer-based formulations for wound healing applications. *European Polymer Journal*, *160*, 110784.

[8] Moholkar, D. N., Sadalage, P. S., Peixoto, D., Paiva-Santos, A. C., & Pawar, K. D. (2021b). Recent advances in biopolymer-based formulations for wound healing applications. *European Polymer Journal*, *160*, 110784.

[9] Mujeeb Rahman, P., Abdul Mujeeb, V. M., Muraleedharan, K., & Thomas, S. K. (2018). Chitosan/nano ZnO composite films: Enhanced mechanical, antimicrobial and dielectric properties. *Arabian Journal of Chemistry*, *11*(1), 120–127. https://doi.org/https://doi.org/10.1016/j.arabjc.2016.09.008

[10] Pensalfini, M., Ehret, A. E., Stüdeli, S., Marino, D., Kaech, A., Reichmann, E., & Mazza, E. (2017). Factors affecting the mechanical behavior of collagen hydrogels for skin tissue engineering. *Journal of the Mechanical Behavior of Biomedical Materials*, *69*, 85–97. https://doi.org/https://doi.org/10.1016/j.jmbbm.2016.12.004

[11] Qian, J., Chen, Y., Yang, H., Zhao, C., Zhao, X., & Guo, H. (2020). Preparation and characterization of crosslinked porous starch hemostatic. *International Journal of Biological Macromolecules*, *160*, 429–436. https://doi.org/https://doi.org/10.1016/j.ijbiomac.2020.05.189

[12] Raguvaran, R., Manuja, B. K., Chopra, M., Thakur, R., Anand, T., Kalia, A., & Manuja, A. (2017). Sodium alginate and gum acacia hydrogels of ZnO nanoparticles show wound healing effect on fibroblast cells. *International Journal of Biological Macromolecules*, *96*, 185–191. https://doi.org/https://doi.org/10.1016/j.ijbiomac.2016.12.009

[13] Rajabi, M., Ali, A., McConnell, M., & Cabral, J. (2020). Keratinous materials: Structures and functions in biomedical applications. *Materials Science and Engineering: C*, *110*, 110612.

[14] Salleh, K. M., & Abd Rashid, N. F. (2024a). Keratin-based biomaterials for biomedical applications. In *Polymer Composites Derived from Animal Sources* (pp. 219–242). Elsevier.

[15] Salleh, K. M., & Abd Rashid, N. F. (2024b). Keratin-based biomaterials for biomedical applications. In *Polymer Composites Derived from Animal Sources* (pp. 219–242). Elsevier.

[16] Sarma, A. (2022). Biological importance and pharmaceutical significance of keratin: A review. *International Journal of Biological Macromolecules*, *219*, 395–413. https://doi.org/https://doi.org/10.1016/j.ijbiomac.2022.08.002

[17] Sellappan, L. K., & Manoharan, S. (2024). Fabrication of bioinspired keratin/sodium alginate based biopolymeric mat loaded with herbal drug and green synthesized zinc oxide nanoparticles as a dual drug antimicrobial wound dressing. *International Journal of Biological Macromolecules*, *259*, 129162. https://doi.org/https://doi.org/10.1016/j.ijbiomac.2023.129162

[18] Shanmugasundaram, O. L., Syed Zameer Ahmed, K., Sujatha, K., Ponnmurugan, P., Srivastava, A., Ramesh, R., Sukumar, R., & Elanithi, K. (2018a). Fabrication and characterization of chicken feather keratin/polysaccharides blended polymer coated nonwoven dressing materials for wound healing applications. *Materials Science and Engineering: C*, *92*, 26–33. https://doi.org/https://doi.org/10.1016/j.msec.2018.06.020

[19] Shanmugasundaram, O. L., Syed Zameer Ahmed, K., Sujatha, K., Ponnmurugan, P., Srivastava, A., Ramesh, R., Sukumar, R., & Elanithi, K. (2018b). Fabrication and characterization of chicken feather keratin/polysaccharides blended polymer coated nonwoven dressing materials for wound healing applications. *Materials Science and Engineering: C*, *92*, 26–33. https://doi.org/https://doi.org/10.1016/j.msec.2018.06.020

[20] Shubha, A., Sharmita, G., & Manaswi, R. (2024). Recent advances in preparation and biomedical applications of keratin based biomaterials. *Biotechnology for Sustainable Materials*, *1*(1), 16.

[21] Vikas, Mehata, A. K., Singh, C., Malik, A. K., Setia, A., & Muthu, M. S. (2024). Alginate-Based Hydrogels as Drug Carriers. In *Biomaterial-based Hydrogels: Therapeutics Carrier and Tissue Regeneration* (pp. 39–65). Springer.

[22] Wang, L., Shang, Y., Zhang, J., Yuan, J., & Shen, J. (2023). Recent advances in keratin for biomedical applications. *Advances in Colloid and Interface Science*, *321*, 103012.

[23] Xie, H., Chen, X., Shen, X., He, Y., Chen, W., Luo, Q., Ge, W., Yuan, W., Tang, X., Hou, D., Jiang, D., Wang, Q., Liu, Y., Liu, Q., & Li, K. (2018). Preparation of chitosan-collagen-alginate composite dressing and its promoting effects on wound healing. *International Journal of Biological Macromolecules*, *107*, 93–104. https://doi.org/https://doi.org/10.1016/j.ijbiomac.2017.08.142

[24] Zhai, M., Xu, Y., Zhou, B., & Jing, W. (2018). Keratin-chitosan/n-ZnO nanocomposite hydrogel for antimicrobial treatment of burn wound healing: Characterization and biomedical application. *Journal of Photochemistry and Photobiology B: Biology*, *180*, 253–258. https://doi.org/https://doi.org/10.1016/j.jphotobiol.2018.02.018